ECOSYSTEM ECOLOGY - ORIGINAL PAPER

Disentangling drought-induced variation in ecosystem and soil respiration using stable carbon isotopes

Stephan Unger · Cristina Máguas · João S. Pereira ·
Luis M. Aires · Teresa S. David · Christiane Werner

Abstract Combining C flux measurements with information on their isotopic composition can yield a process-based understanding of ecosystem C dynamics. We studied the variations in both respiratory fluxes and their stable C isotopic compositions ($\delta^{13}C$) for all major components (trees, understory, roots and soil microorganisms) in a Mediterranean oak savannah during a period with increasing drought. We found large drought-induced and diurnal dynamics in isotopic compositions of soil, root and foliage respiration ($\delta^{13}C_{res}$). Soil respiration was the largest contributor to ecosystem respiration (R_{eco}), exhibiting a depleted isotopic signature and no marked variations with increasing drought, similar to ecosystem respired $\delta^{13}CO_2$, providing evidence for a stable C-source and minor influence of recent photosynthate from plants. Short-term and diurnal variations in $\delta^{13}C_{res}$ of foliage and roots (up to 8 and 4‰, respectively) were in agreement with: (1) recent hypotheses on post-photosynthetic fractionation processes, (2) substrate changes with decreasing assimilation rates in combination with increased respiratory demand, and (3) decreased phosphoenolpyruvate carboxylase activity in drying roots, while altered photosynthetic discrimination was not responsible for the observed changes in $\delta^{13}C_{res}$. We applied a flux-based and an isotopic flux-based mass balance, yielding good agreement at the soil scale, while the isotopic mass balance at the ecosystem scale was not conserved. This was mainly caused by uncertainties in Keeling plot intercepts at the ecosystem scale due to small CO_2 gradients and large differences in $\delta^{13}C_{res}$ of the different component fluxes. Overall, stable isotopes provided valuable new insights into the drought-related variations of ecosystem C dynamics, encouraging future studies but also highlighting the need of improved methodology to disentangle short-term dynamics of isotopic composition of R_{eco}.

Communicated by Dan Yakir.

S. Unger (✉) · C. Werner
Department of Experimental and Systems Ecology,
University of Bielefeld, Universitätsstrasse 25 (W4-114),
33615 Bielefeld, Germany
e-mail: stephan.unger@uni-bielefeld.de

C. Máguas
Centro de Ecologia e Biologia Vegetal, Faculdade de Ciências,
Universidade Lisboa, Campo Grande, 1749-016 Lisbon, Portugal

J. S. Pereira
Instituto Superior de Agronomia, Universidade Técnica
de Lisboa, Tapada da Ajuda, 1349-017 Lisbon, Portugal

L. M. Aires
CESAM, Departamento de Engenharia do Ambiente,
Escola Superior de Tecnologia e Gestão,
Instituto Politécnico de Leiria, Campus 2,
2411-901 Leiria, Portugal

T. S. David
Instituto Nacional de Recursos Biológicos, I.P.,
Quinta do Marquês, 2780-159 Oeiras, Portugal

Abbreviations

$\delta^{13}C$	Isotopic composition (of respired CO_2)
R	Respiratory flux
R_{eco}	Ecosystem respiratory signal
res	Respiratory signal of ecosystem components
S	Soil
C	Canopy
T	Trees

U	Understory plants
SMO	Soil microorganisms
r	Roots and associated symbionts

Introduction

Ecosystem respiration (R_{eco}) is one of the major determinants of the C balance in most terrestrial ecosystems (Valentini et al. 2000). Global warming impacts on ecosystem moisture and temperature patterns might induce substantial changes in R_{eco} (e.g., Huxman et al. 2003; Xu et al. 2004; Davidson et al. 2006). Thus, having a process-based understanding of R_{eco}, particularly in response to a changing climate, is desirable although difficult to achieve since different C pools and respiratory sources (e.g., autotrophic and heterotrophic respiration) respond differentially to changes in the abiotic environment.

Stable C isotopes are used extensively to examine respiratory processes and their environmental drivers (e.g., Bowling et al. 2008), adding invaluable information on substrate turnover, C metabolism as well as photosynthetic and post-photosynthetic fractionation processes imprinted in the isotopic signature of respired CO_2. However, so far a complete understanding of the isotopic composition of C pools and fluxes in terrestrial ecosystems has not been achieved (Bowling et al. 2008). The stable C isotopic composition ($\delta^{13}C$) of ecosystem respired CO_2 ($\delta^{13}C_R$) is an important parameter for application in isotope-based C budget models and understanding the controls over terrestrial C exchange processes (e.g., McDowell et al. 2004a). $\delta^{13}C_R$ is known to vary seasonally with changes in photosynthetic discrimination and respiratory activity (e.g., Bowling et al. 2001, 2002; Griffis et al. 2004; Ponton et al. 2006; Werner et al. 2006, 2007a; Alstad et al. 2007; Schaeffer et al. 2008). Recent studies showed small (Ogée et al. 2003; Still et al. 2003; Schnyder et al. 2004) to large (>6‰; e.g., Bowling et al. 2003; Werner et al. 2006; Kodama et al. 2008) variation in $\delta^{13}C_R$ even within a single night. Still, a general understanding of the causes of this variability in $\delta^{13}C_R$ has not yet been achieved and the interplay of processes driving R_{eco} remains largely unknown. Changes in either the magnitude of component fluxes or their isotope composition ($\delta^{13}C_{res}$) may drive the observed variations in the isotopic signature of $\delta^{13}C_R$. Substantial temporal variations in isotopic composition of CO_2 respired by leaves (e.g., Hymus et al. 2005; Mortazavi et al. 2005; Kodama et al. 2008; Werner et al. 2007b, 2009; Priault et al. 2009; Sun et al. 2009), roots (e.g., Klumpp et al. 2005), and soils (e.g., McDowell et al. 2004a; Ekblad et al. 2005; Kodama et al. 2008) have been observed. Variability in photosynthetic discrimination is thought to

largely determine the isotopic composition of plant as well as soil and even R_{eco} (e.g., Ekblad and Högberg 2001; Bowling et al. 2002; Mortazavi et al. 2005; Werner et al. 2006). Another reason for the variation in $\delta^{13}C_{res}$ and $\delta^{13}C_R$ might be temporal changes in C supply by assimilation that could bring about changes in the utilization of different respiratory substrates (e.g., old vs. new C; Nogués et al. 2006). Additionally, there is now evidence for substantial metabolic fractionation in the dark respiratory pathways of leaves (e.g., Rossmann et al. 1991; Gleixner and Schmidt 1997; Tcherkez et al. 2003; Ghashghaie et al. 2003; Mortazavi et al. 2006; Werner et al. 2007b, 2009; Barbour and Hanson 2009; Priault et al. 2009) and during C transport and allocation to stem and roots (Gleixner and Schmidt 1997; Tcherkez et al. 2004; Brandes et al. 2006; Gessler et al. 2009a; Cernusak et al. 2009). Thus, apart from the differential climatic dependencies that bring about changes in magnitude and isotope composition of plant, soil and root respiration fluxes, metabolic processes occurring in each of these components will also have isotope effects which may influence $\delta^{13}C_R$. Determining how stable isotope compositions vary in component fluxes and how they affect $\delta^{13}C_R$ can provide a better process-based understanding of ecosystem C exchange dynamics. No study has yet measured the $\delta^{13}C$ values of R_{eco} and all components simultaneously, while only a few have measured several of these fluxes at once (Bowling et al. 2008).

Due to their marked seasonality and assorted periods of rapid changes in net C exchange and their simple two-layer structure, Mediterranean oak woodlands ('montado') provide excellent conditions for the examination of diurnal and short-term temporal dynamics in ecosystem component $\delta^{13}C_{res}$ and their effects on $\delta^{13}C_R$. Drought is the major constraint for plant productivity in the Mediterranean (e.g., Tenhunen et al. 1990; Pereira et al. 2007) and the rapid climatic transition from spring to summer drought induces a large shift in ecosystem CO_2 exchange in a relatively short time frame. During this period the rapidly declining contribution of the understory is of special relevance for the net ecosystem C flux, as we previously showed in an ecosystem-scale flux partitioning study (Unger et al. 2009). We concluded that the R_{eco} flux depends on the interplay of all contributing fluxes [trees, understory, soil microorganisms (SMO) and roots] and thus that its isotopic composition ($\delta^{13}C_R$) should vary in accordance with changes in the contributions and isotopic signatures of the component fluxes. The present study aims firstly, to explain variation in $\delta^{13}C_R$ with variation in both isotopic signatures and respiratory fluxes of the different ecosystem components (soil, roots, understory and tree foliage) and secondly, to achieve a process-based interpretation of drought-induced and diurnal variation in

the isotopic signature of these components. We monitored variability in both $\delta^{13}C_{res}$ and $\delta^{13}C_R$ to add this information to the C flux partitioning presented in Unger et al. (2009). We addressed the following hypotheses: (1) drought-induced processes such as altered photosynthetic discrimination and respiratory demands will cause substantial changes in both ecosystem and component respired $\delta^{13}CO_2$, and (2) the feedbacks of the isotopic compositions of the component fluxes (soils, foliage, roots) on $\delta^{13}C_R$ and $\delta^{13}C_S$ can be reproduced in an isotopic mass balance.

Materials and methods

Field site and climatic conditions

The experimental site Mitra (CarboEurope–IP) near Évora in southern Portugal (38°N; 8°W) has a typical Mediterranean climate, with hot and dry summers and mild wet winters. The mean annual temperature is 15–16°C and average annual precipitation is ca. 669 mm. The site is located in a homogeneous landscape (220–250 m a.s.l.) dominated by savannah-like woodlands with drought-adapted evergreen *Quercus ilex* ssp. *rotundifolia* L. and *Quercus suber* L. (Werner and Correia 1996) growing on sandy soils derived from granite rock. The understory consists of grazed pasture dominated by drought-sensitive herbaceous annuals [e.g., *Tuberaria guttata* (L.) Fourr.], some Gramineae and a few drought-deciduous shrubs (*Cistus salvifolius* L.). Tree canopy cover is about 21% and leaf area index ca. 0.55 (Carreiras et al. 2006). The vegetative period of the understory lasts from the autumn rains until May–June when soil water content (SWC) generally decreases rapidly. Measurements were conducted between 20 May and 3 June 2006. For C flux partitioning between understory and tree canopy we used understory flux data from Tojal, a grassland adjacent to the Mitra field site (8 km distance, CarboEurope–IP) at the same altitude, with the same soil type and climate as Mitra (Pereira et al. 2007). Vegetation was mainly C3 grasses that were also found in the oak site and one additional C4 species (*Cynodon dactylon* L.; Pereira et al. 2007). Furthermore, seasonality and leaf duration are similar between the oak woodland understory and grassland (Pereira et al. 2007) and annual courses of gross primary production (GPP) and R_{eco} are highly correlated between the sites. The grassland had been mown on 24 May 2006. However, the cut biomass was mainly dead dry leaf matter (Aires et al. 2008) thus had little influence on the understory respiration flux. Further, the cut dry leaf matter was left on the field, thus the shade effect on the soil was not significantly reduced.

Eddy covariance and micrometeorological measurements

Continuous records of CO_2 and H_2O fluxes and climate variables were taken on a 28-m-high metal tower (at the Mitra site) equipped with a sonic anemometer (Gill R3; Gill Instruments, Lymington, Hampshire, UK) and a gas analyzer (LI-7000; LI-COR, Lincoln, NE, USA). Weather conditions were continuously recorded by a meteorological station (datalogger CR10X; Campbell Scientific, Logan, UT, USA), with a Q7 REBS net radiometer (Campbell Scientific), aspirated psychrometer H301 (Vector Instruments, Rhyl, Denbighshire, UK) and a rainfall recorder (tipping-bucket rain gauge; Casella, Bedford, UK). Understory fluxes at the Tojal grassland site were measured by a small eddy covariance system at a height of 2.5 m (3D sonic anemometer, 1210R3; Gill Instruments; IRGA, LI-COR) at Tojal, a grassland adjacent to the Mitra field site (CarboEurope–IP).

Eddy covariance data were processed using Eddyflux software (Meteotools, Jena, Germany). Following the CarboEurope-IP recommendations, a planar fit coordinate rotation for wind components was performed. The quality of all primary data was guaranteed by a routine equipment calibration and, for meteorological data, a comparison with data from other nearby stations. Flux-partitioning methods proposed by Reichstein et al. (2005) were applied to separate the net ecosystem exchange into GPP and R_{eco}, respectively. During the 2-week study period there was no missing eddy covariance or climate data. For a detailed description of the eddy covariance data processing and flux partitioning see Unger et al. (2009).

Plant-scale observations

Leaf gas exchange (LI-6400; LI-COR) was recorded in 24-h cycles every 2–4 h on marked branches, for at least three sun-exposed leaves on three *Q. ilex* trees and on ten sun exposed *T. guttata* plants. During daytime dark leaf respiration was measured by covering the cuvette with a black plastic shield. This procedure did not affect leaf temperature. Predawn and midday leaf water potentials (pressure chamber; Manofrigido, Portugal) were also obtained for the same species.

Soil respiration measurements and trenching

Soil respiration (R_S) was measured in 24-h cycles every 2–4 h using a closed path chamber system (PP-System EGM2 soil respiration system with SRC-1 chamber; PP-Systems, Amesbury, MA, USA). Measurements were conducted with three replicates on three plots of untreated bare soil and three plots with root exclusion. Root exclusion was

achieved by inserting metal rings (30 cm diameter) from 0 to 20 cm depth (trenching) and covering them with black foil (solarization) for 2 weeks, 1 year prior to measurements to avoid effects of disturbance or decomposition of decaying root material (e.g., Lee et al. 2003). We regarded trenching up to 20 cm depth as sufficient for the studied site, since the upper soil layer contains the largest fraction of root biomass (Kurz-Besson et al. 2006). Plots were installed 20 m from the nearest tree. Thus, the contribution of respiration from deep tree roots was regarded as negligible. Three weeks before measurements a few new seedlings inside the trenching plots were carefully removed and solarization was repeated to ensure root-free plots. Soil temperature (T_{soil}) and SWC were recorded at 5- to 10-cm depth alongside R_S using the temperature sensor of the soil respiration system and a moisture probe (Theta Meter HH1; Delta-T Devices, Cambridge, UK).

Air sampling and isotopic analysis

We used 12-ml soda glass vials (Exetainer; Labco, High Wycombe, UK) capped with pierceable septa for atmospheric air sampling (Werner et al. 2007b). Samples for Keeling plot analyses were collected during four 24-h cycles with one measurement series every 2–3 h. Air was collected at nine heights: 24, 20, 16, 12, 8, 4, 2, 1 and 0.5 m (the heights between 16 and 24 m were above the tree canopy). Air was pumped at 10 l min^{-1} (pump Capex V2X; Charles Austen Pumps, Byfleet, Surrey, UK) through Dekarbon tubing (25 m length, inner diameter 6.9 mm; Sertoflex, Serto Jacob, Fuldabrück, Germany), which was fixed at the tower. A simple sampling system consisting of an Exetainer vial pierced by two needles connected to the pump and an infrared gas analyzer (IRGA; BINOS 100 4P, Rosemount Analytical, Hanau, Germany; precision for CO_2 ±1 p.p.m.) was mounted, and pumped air through the tubing until stable CO_2 concentrations were reached; it then sampled for 1 min. Samples were repeatedly collected from the top to the bottom for 30 min resulting in two to three samples per height.

$\delta^{13}C_{res}$ of R_S was estimated by chamber Keeling plots. The same pump and IRGA were connected with Dekarbon tubing to a well-ventilated and gas-tight cylindrical Plexiglas chamber (17 l, diameter 30 cm) in a closed system. Temperature and light levels inside the chamber were monitored with two thermocouples fixed at different heights and a quantum sensor, connected to a datalogger (CR10; Campbell Scientific). The chamber was tightly fitted on a metal ring inserted in the soil and sealed with acryl rubber mastic. Air was sampled every minute, while CO_2 concentrations inside the chamber were rising; a total of ten samples per soil Keeling plot was collected.

For collection of leaf and root respired CO_2, ten leaves of *Q. ilex* as well as ten leaves and ten root fragments of *T. guttata* were cut and immediately placed into exetainers which were flushed with CO_2-free air (passed through a soda lime column and monitored by IRGA) and incubated for 10 min in a temperature-isolated plastic box (see Werner et al. 2007b). A validation of the method with online-gas exchange measurements on intact leaves revealed no difference in $\delta^{13}C_{res}$ in comparison to cut leaves (see Werner et al. 2007b). Respired CO_2 was collected with a 25-ml gas-tight syringe (SGE International, Victoria, Australia) from the exetainer and injected into a second CO_2-free exetainer, with rapid needle removal following injection. Tests revealed no significant differences in $\delta^{13}CO_2$ before and after the syringe transfer (SD < 0.15‰). Additionally, five vials of known $\delta^{13}C$ and CO_2 concentration were filled in the field at each sampling date and used as references. Samples were analyzed (UAI, ICAT, Lisbon, Portugal) within 12–20 h after collection. Isotopic compositions were measured with a stable isotope ratio mass spectrometer (IsoPrime; GV Instruments, Manchester, UK) operating in continuous-flow mode coupled to a Multiflow prep-system (GV Instruments). A laboratory gas of known isotopic composition was measured to correct for any drift. Repeated measurement precision was <0.1‰.

Keeling plot calculation

The Keeling plot approach was used to assess the isotopic composition of ecosystem and soil respired CO_2. Assuming that both source and background CO_2 remain constant during the sampling period (<30 min), the isotopic signature of R_{eco} ($\delta^{13}C_R$) can be calculated as the y-intercept of a linear regression of $\delta^{13}C$ versus the inverse of the CO_2 mixing ratio obtained from vertical profiles (Keeling 1958):

$$\delta^{13}C_a = c_T(\delta^{13}C_T - \delta^{13}C_R)(1/c_a) + \delta^{13}C_R \qquad (1)$$

where $\delta^{13}C$ denotes isotopic composition and c denotes CO_2 concentrations of the mixing ratios. The subscripts indicate air samples from several heights above and within the canopy (a), tropospheric air (T) and air respired from the ecosystem (R). We calculated ordinary least square (model I; Zobitz et al. 2006) and geometric mean (model II) regressions (Pataki et al. 2003) and did not find significant variation between model I and model II results, when CO_2 gradients were above 30 p.p.m. Presented data are from model I regressions following current practice (Zobitz et al. 2006). To remove outliers, residual analyses were performed. Data points were removed from the regression when the residual of an individual data point was greater than 3 times the SD. Regressions were rejected when not significant ($\alpha = 0.01$). Uncertainties in the Keeling plot

intercepts were expressed as SEs of the intercept. Statistical and regression analyses were performed using Statistica (StatSoft, Tulsa, OK, USA) and JMP (SAS Institute, Cary, NC, USA).

Flux partitioning

For nighttime flux partitioning a mass balance equation was applied (Eq. 2; henceforth called the 'ecoflux' approach), which assumes that the sum of component fluxes equals the ecosystem flux and that no other component fluxes than soil flux (roots and SMO) and canopy flux (leaves of trees and herbs) contribute to the ecosystem flux:

$$R_{eco} = R_S + R_C = R_r + R_{SMO} + R_T + R_U \qquad (2)$$

where R denotes the respiratory CO_2 flux per square meter ground. Subscripts indicate respired CO_2 from ecosystem (eco), soil (S), canopy (C), roots (r), SMO as well as from tree (T) and understory leaves (U). Respiration from non-mycorrhizal fungi and microbes is included in heterotrophic R_S (R_{SMO}), whereas autotrophic R_S (R_r) flux comprises root respiration and associated rhizospheric components (e.g., mycorrhizal respiration). Nighttime R_{eco} (measured) minus the soil flux (R_S, measured) yields the canopy respiration flux (R_C; comprising trees and understory). Subtracting R_S of trenching plots (R_{SMO}, measured) from the total soil flux (R_S, measured) yields the root flux (R_r). The nighttime respiration flux from understory eddy covariance data (see Eddy covariance and micrometeorological measurements) was used to partition R_S from understory respiration (R_U). Tree respiration (R_T) was then calculated by subtracting R_U from R_C. We then added stable isotope information to Eq. 2 yielding an isotopic flux mass balance ('eco-isoflux' approach, Eq. 3):

$$\begin{aligned}
\delta^{13}C_R \times R_{eco} &= \left(\delta^{13}C_S \times R_S\right) + \left(\delta^{13}C_C \times R_C\right) \\
&= \left(\delta^{13}C_r \times R_r\right) + \left(\delta^{13}C_{SMO} \times R_{SMO}\right) \\
&\quad + \left(\delta^{13}C_T \times R_T\right) + \left(\delta^{13}C_U \times R_U\right)
\end{aligned} \qquad (3)$$

where $\delta^{13}C$ denotes isotopic composition (subscripts as in Eq. 2).

Apart from $\delta^{13}C_C$ we measured all isotopic compositions entering Eq. 3 directly: $\delta^{13}C_R$ was measured by the Keeling plot method at the eddy flux tower (see above), $\delta^{13}C_S$ and $\delta^{13}C_{SMO}$ were measured on separate plots (trenched and not trenched, see above), while $\delta^{13}C_T$, $\delta^{13}C_U$ and $\delta^{13}C_r$ were measured from leaves (trees and understory) and roots (understory) by the in-tube incubation method (see above). Flux measurements were obtained as described above for Eq. 2. We used these measurements to rearrange Eq. 3 in order to compare the results of eco-isoflux and ecoflux approaches (Eq. 2). For example, to obtain R_{eco} from the eco-isoflux approach we rearranged

Eq. 3 by division with $\delta^{13}C_R$ and compared this value with the measured R_{eco}.

Since root respiration was calculated exclusively from R_S, both flux and isoflux partitioning could also be applied independently from R_{eco} at the soil scale ('soilflux', Eq. 4 and 'soil-isoflux', Eq. 5):

$$R_S = R_r + R_{SMO} \qquad (4)$$

$$\delta^{13}C_S \times R_S = \left(\delta^{13}C_r \times R_r\right) + \left(\delta^{13}C_{SMO} \times R_{SMO}\right) \qquad (5)$$

To quantify the degree of uniformity between eco-isoflux (soil-isoflux) and ecoflux (soilflux) mass balances, we linearly correlated data from the different approaches and calculated an average offset (AO; %) between the measured and the isotope mass balance data. Correlation coefficients (R^2) give information on similar trends, while the AO indicates differences in the data range.
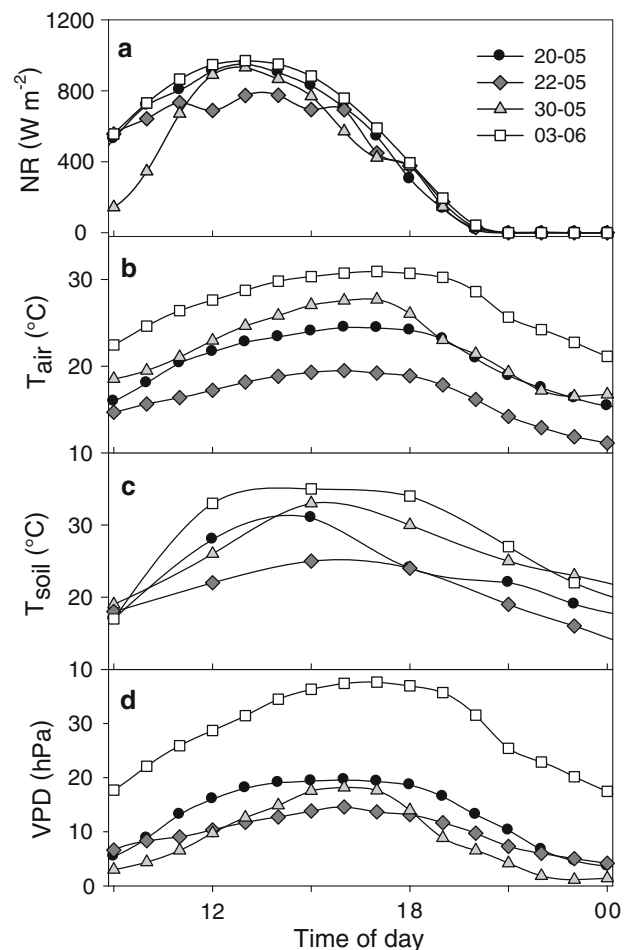

Fig. 1 Diurnal variation in **a** net radiation (*NR*), **b** air temperature (*T*$_{air}$), **c** soil temperature (*T*$_{soil}$; 5-cm depth) and **d** vapor pressure deficit (*VPD*) for 20 May (*black circles*), 22 May (*dark-grey diamonds*), 30 May (*light-grey triangles*) and 3 June (*white squares*) 2006

Results

Variation in climatic variables and respiration fluxes

Meteorological conditions during spring 2006 were typical for the Mediterranean climate with highest precipitation in March (104 mm) and April (57 mm) and continuously increasing air temperature (T_{air}), net radiation and vapor pressure deficit (VPD). The last rainfall was on 22 April. Hence, when measurements were conducted at the end of May, the herbaceous vegetation already showed signs of water deficit.

Most days were sunny, except for 22 May with rather cloudy conditions (Fig. 1a). Maximum T_{air} and VPD were 31°C and to 36 hPa, respectively (Fig. 1b, d). T_{soil} followed the same pattern as T_{air}, but revealed slightly higher values (Fig. 1c).

Leaf gas exchange and water potential measurements on trees (*Q. ilex*) and understory plants (*T. guttata*) reflected a differential response to increasing water deficit and

Table 1 Net photosynthesis (*NP*) rates, predawn and midday leaf water potentials (*WP*) of trees (*Quercus ilex*) and understory plants (*Tuberaria guttata*) during late spring 2006. $n = 3$–10 ($\pm$ SD)

	20 May	22 May	30 May	3 June
Q. ilex				
$WP_{predawn}$ (MPa)	-0.3 ± 0.2	-0.5 ± 0.1	-0.6 ± 0.2	-0.7 ± 0.1
WP_{midday} (MPa)	-1.6 ± 0.1	-2.0 ± 0.2	-2.9 ± 0.2	-2.8 ± 0.2
NP (μmol m^{-2} s^{-1})	2.8 ± 0.9	4.4 ± 1.0	3.5 ± 0.8	4.6 ± 0.7
T. guttata				
$WP_{predawn}$ (MPa)	-0.5 ± 0.1	-0.6 ± 0.1	-1.1 ± 0.1	-1.5 ± 0.4
WP_{midday} (MPa)	-1.5 ± 0.1	-1.6 ± 0.1	-1.9 ± 0.3	-2.2 ± 0.3
NP (μmol m^{-2} s^{-1})	1.8 ± 0.7	2.0 ± 0.7	1.7 ± 0.7	-2.1 ± 0.7

Fig. 2 Temporal variation in **a–d** single-leaf respiration (R_{leaf}) of *Quercus ilex* (*grey triangles*), **e–h** R_{leaf} of *T. guttata* (*grey inverted triangles*), **i–l** respiration fluxes from soil (R_{soil}; *black circles*), soil microorganisms (SMO) (R_{SMO}; *grey hexagons*), roots (R_{root}; *white diamonds*) and **m–p** ecosystem respiration (R_{eco}; *grey squares*) for four diurnal cycles with increasing summer drought (May–June 2006). Note: foliage flux values (**a–h**) are given in m^2 leaf area. *Black bars* indicate nighttime; $n = 3$–5 ($\pm$ SE)
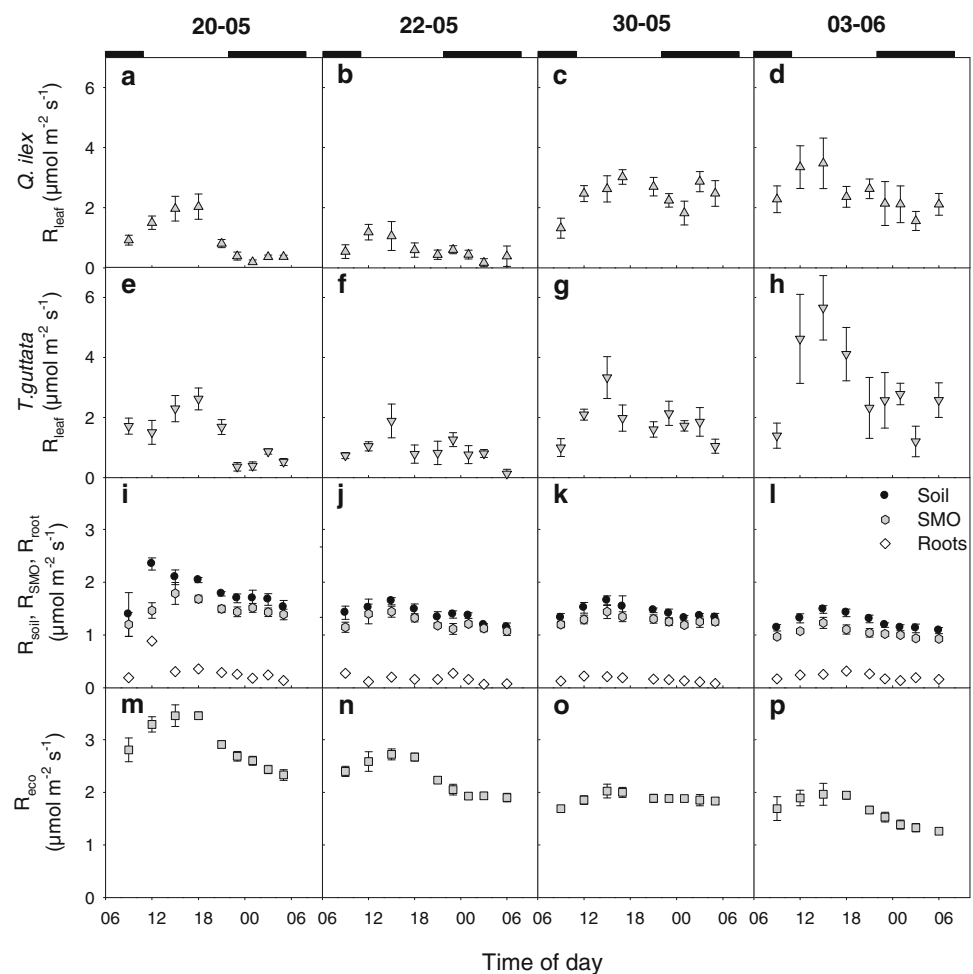
temperature (Table 1; Fig. 2a–h). While *Q. ilex* was able to preserve predawn leaf water potentials around −0.5 MPa and maintained net photosynthesis rates of ∼3–4 μmol m^{-2} s^{-1} (Table 1), understory plants like *T. guttata* were severely affected by seasonal drought and died off during the study period. Predawn leaf water potentials became increasingly similar to midday values (−1.5 MPa) and generally low net photosynthesis turned into net respiration towards 3 June (Table 1). Dark respiration rates of leaves revealed a clear diurnal cycle and increased strongly with drought in both species (Fig. 2a–h), particularly in *T. guttata* (up to 6 μmol m^{-2} s^{-1}; Fig. 2h). Please note that leaf gas exchange measurements were always performed on live green foliage. Thus, the increasing respiration rates do not contrast with ecosystem-scale measurements, where understory respiration decreased due to strong wilting effects causing a decline in leaf area.

R_S showed a slight decrease (∼1 μmol m^{-2} s^{-1}) in response to seasonal drought and exhibited higher rates during daytime than during nighttime (Fig. 2i–l). Soil microorganism respiration showed slightly smaller rates but a similar pattern to total soil efflux, whereas root respiration exhibited little variation over the observed period with consistently low rates of about 0.2 μmol m^{-2} s^{-1} (Fig. 2i–l).

R_{eco} decreased from 3.5 to 1.5 μmol m^{-2} s^{-1} (Fig. 2m–p) and showed similar diurnal dynamics to R_S.

Variation in isotopic composition of respired CO_2

Respired $\delta^{13}CO_2$ of plant material was substantially more enriched than R_S. $\delta^{13}C_{res}$ of *Q. ilex* leaves varied around −19.8 ± 1.2‰ on 20 May and exhibited a continuous decrease to −22.1 ± 0.6‰ throughout the experiment (Fig. 3a–d). The same tendency was observed in leaves of *T. guttata* but the decrease in $\delta^{13}C_{res}$ was even stronger, from −21.3 ± 1.3 to −25.9 ± 1.7‰, whereas roots of *T. guttata* exhibited only a small decrease, from −21.8 ± 1.5 to −22.9 ± 1.7‰ (Fig. 3e–h).

On a diurnal scale, leaf dark $\delta^{13}C_{res}$ was more enriched during the day than at night in both species. Maximum observed variation in $\delta^{13}C_{res}$ was 1.7, 4.2 and 4.8‰ during the daytime and 3.3, 4.6 and 3.8‰ during the nighttime in *Q. ilex* leaves, *T. guttata* leaves and roots,

Fig. 3 Diurnal cycles of stable C isotopic composition ($\delta^{13}C$) of respired CO_2 ($\delta^{13}C_{res}$) from **a–d** *Q. ilex* leaves (*grey triangles*), **e–h** *T. guttata* leaves (*grey inverted triangles*) and roots (*white diamonds*), **i–l** soil (*black circles*) and SMO (*grey circles*) and **m–p** ecosystem respiration ($\delta^{13}C_R$) derived from Keeling plots (*grey squares*) and the eco-isoflux approach (*crosses*) during May and June 2006. *Black bars* indicate nighttime; $n = 10$ (± SE)
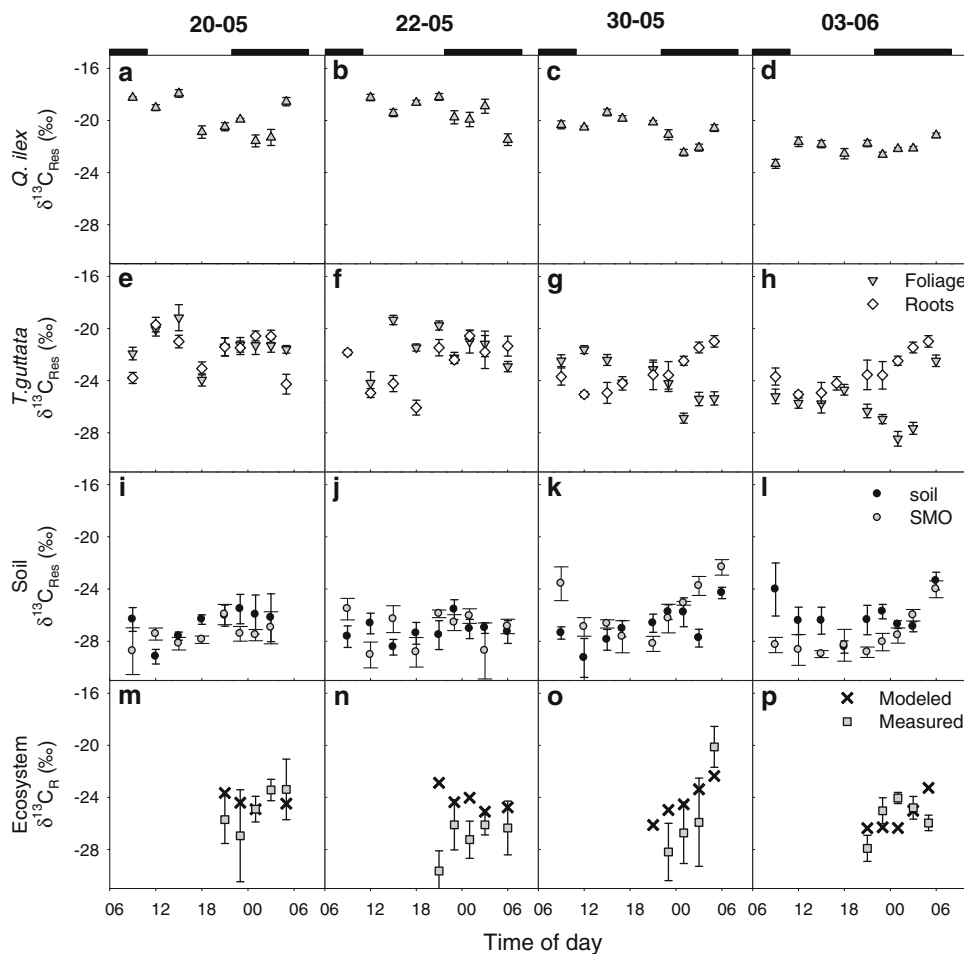
respectively. Maximum differences between day and night were 3.6 and 5.3‰ in *Q. ilex* and *T. guttata*, respectively. The diurnal amplitude in *Q. ilex* $\delta^{13}C_{res}$ decreased with drought.

With increasing drought roots of *T. guttata* exhibited a pattern opposite to that of leaves, showing progressive enrichment during night (Fig. 3e–h). The largest differences between $\delta^{13}C_{res}$ of leaves and roots (up to 7‰) were found on the night of 3 June (Fig. 3h). $\delta^{13}C_{res}$ of R_S did not change significantly over time and was on average -26.8 ± 1.2‰ (Fig. 3i–l), with no distinct diurnal pattern. Heterotrophic R_S constituted the largest fraction of overall R_S and $\delta^{13}C_{res}$ from root-free plots was similar to that from intact soil. However, under progressive drought there was some diel variability in $\delta^{13}C_{res}$ of SMO with a nocturnal increase in $\delta^{13}C_{res}$ on the last 2 sampling days (Fig. 3k, l), similar to the pattern observed for root respiration (Fig. 3g, h).

Isotopic composition of R_{eco} ($\delta^{13}C_R$) showed, apart from $\delta^{13}C_{res}$ of soil and SMO, the most depleted values (on average -25.9 ± 2.1‰; Fig. 3m–p). Further, we observed a strong nocturnal enrichment in $\delta^{13}C_R$ ranging between 2 and 4‰ (7.2‰ on 30 May; Fig. 3o). With increasing drought mean $\delta^{13}C_R$ values became slightly enriched (-27.3 ± 1.4 to -25.3 ± 1.4‰) and the amplitude in the nocturnal cycle decreased from on average 5.7 ± 1.7 to 3.6‰. However, given the large SEs of the intercepts these trends must be interpreted with care. $\delta^{13}C_R$ estimated by the eco-isoflux approach was in the range of measured $\delta^{13}C_R$ but in comparison exhibited slightly enriched values (on average -24.6 ± 1.2‰; Fig. 3m–p). Deviations between measured and estimated $\delta^{13}C_R$ were partially large (in one case up to 6‰; Fig. 3n) and on average ca. 2‰. There was a weak, though not significant, correlation between the SEs in the Keeling plot intercepts and the differences of measured and eco-isoflux estimated $\delta^{13}C_R$ ($R^2 = 0.13$).

Fig. 4 Temporal changes in measured and scaled fluxes from **a** R_{eco} (*squares*), **b** R_{soil} (*circles*), **c** tree respiration (*triangles*), **d** R_{root} (*diamonds*), **e** understory respiration (*inverted triangles*) and **f** R_{SMO} (*hexagons*); measured and ecoflux values, *grey symbols with lines*; eco-isoflux values, *black symbols*; soil-isoflux values, *white symbols*. Note: apart from R_{soil}, all respiration flux partitioning was generally during nighttime and foliage flux values are given in m^2 ground and not leaf area. All isotope data entering the eco-isoflux mass balance are measured values. *Black bars* indicate nighttime. For abbreviations, see Fig. 2
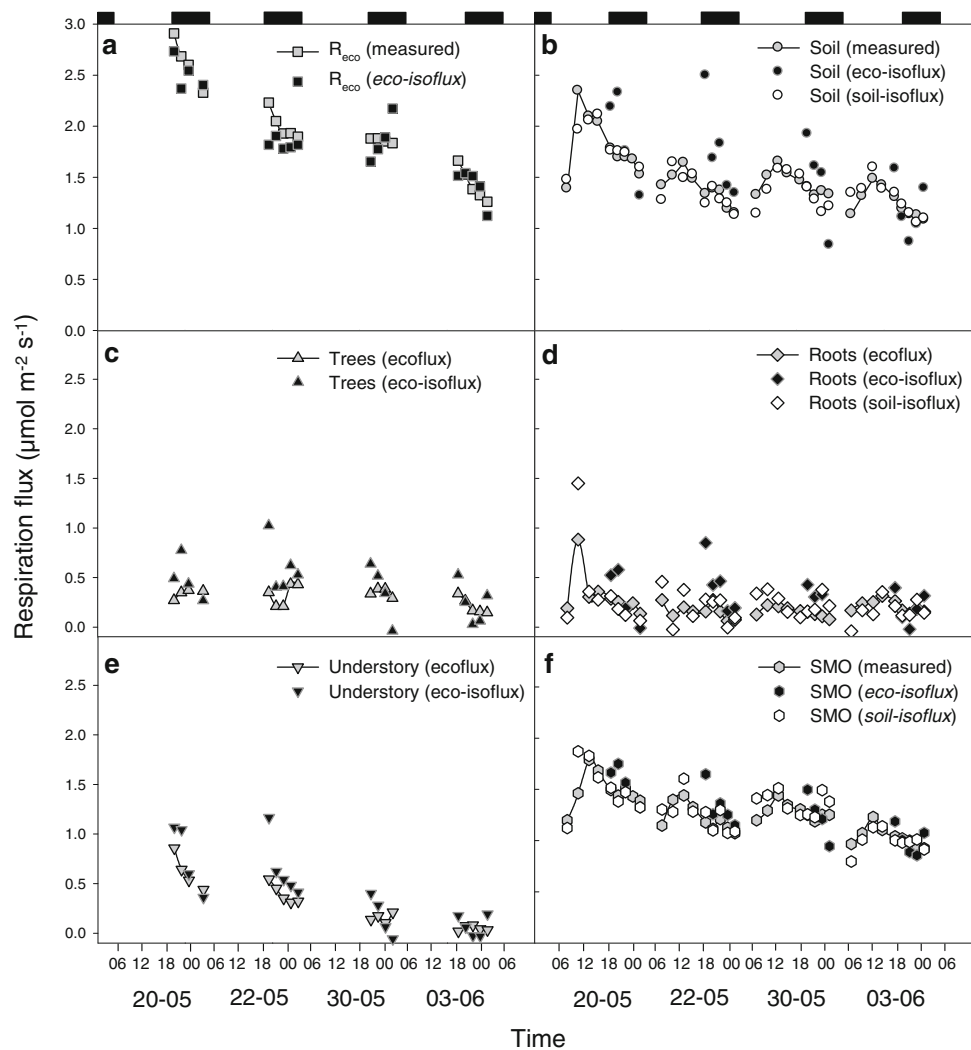
Table 2 Correlation coefficients (R^2) and average offset between correlated data points (AO; %) for correlations of measured and ecoflux estimated respiration fluxes (R) from ecosystem and ecosystem components [trees, understory, soil, soil microorganisms (SMO), roots] with the respective isotopic flux mass balances (eco-isoflux and soil-isoflux); $n = 20$

	R_{eco} (measured)		R_T (ecoflux)		R_U (ecoflux)		R_S (measured)		R_{SMO} (measured)		R_r (ecoflux)	
	R^2	AO	R^2	AO	R^2	AO	R^2	AO	R^2	AO	R^2	AO
Eco-isoflux	0.72	8	0.02	75	0.66	59	0.21	31	0.3	14	0.33	187
Soil-isoflux	–	–	–	–	–	–	0.81	6	0.69	8	0.77	64

Partitioning of isotopic fluxes and comparison of different partitioning approaches

To evaluate changes in the contribution of component fluxes to total R_{eco} with increasing water deficit and temperature, we used two different partitioning approaches, based on measured fluxes (ecoflux approach, Eq. 2) and their respective isotopic signatures (eco-isoflux approach, Eq. 3). A main outcome of the ecoflux partitioning is that the drought-sensitive understory species play the most important role in causing the rapid decrease in R_{eco}, the latter thus becoming increasingly dominated by heterotrophic R_S. The results of the ecoflux approach have been discussed in Unger et al. (2009). Including stable isotopes in the mass balance (eco-isoflux approach), however, revealed partially different results.

To test the eco-isoflux approach for consistency, we solved the mass balance presented in Eq. 3 for the flux rates of all individual components (Fig. 4). We found that not all measured fluxes and corresponding isotope ratios led to a sensible solution of the mass balance. The most reasonable solution was achieved using isofluxes from $\delta^{13}C_{res}$ of soil, herbs and tree respiration and their respective measured fluxes and measured $\delta^{13}C_R$ data to solve Eq. 3 for R_{eco}. In contrast, when using measured $\delta^{13}C_R$ in the eco-isoflux approach we detected significant deviations in the calculated component fluxes from those obtained by the ecoflux approach. This deviation was larger when the estimated component flux was small (Table 2; Fig. 4). Thus, the highest agreement (i.e., highest correlation and lowest offset) between the eco-isoflux and the ecoflux approach was achieved for R_{eco} ($R^2 = 0.72$; AO = 8%; see Table 2; Fig. 4a), while largest deviations were found for the smallest component fluxes ($R^2 = 0.33$ and 0.02 for root and tree respiration see Table 2; Fig. 4c, d). Further, non-congruencies of summed mass balance estimates from R_{root} and R_{SMO} magnified the difference between ecoflux and eco-isoflux mass balance for R_S, resulting in low correspondence between the approaches ($R^2 = 0.21$; AO = 31%; see Table 2; Fig. 4b).

Since respiration of soil, roots and SMO was measured independently of the ecosystem fluxes we were able to compare the different partitioning approaches exclusively at the soil scale (soil-isoflux approach; Eq. 5; Fig. 4b, d, f): root respiration calculated by soil-isoflux partitioning was in the same range and followed nicely the pattern of the ecoflux approach (Fig. 4d; Table 2). Outliers were only observed for the midday value of 20 May, where isoflux partitioning overestimated the root flux. Given that the root respiration flux was very small (<0.5 μmol m^{-2} s^{-1}) these outliers are negligible. Respiration fluxes from total soil and SMO as estimated by the soil-isoflux approach revealed high agreement with the soilflux approach (Eq. 4; Fig. 4b, f; Table 2).

Discussion

The presented approach combines understory versus overstory C flux partitioning with the additional information provided by stable isotopes. We will discuss the potential mechanisms underlying the observed drought effects on R_{eco} by disentangling the possible causes of variation in $\delta^{13}C_{res}$ of the main ecosystem components. Further, we will discuss the benefits and limitations of including stable C isotopes in a flux-based mass balance at both soil and ecosystem scales.

Variation in $\delta^{13}C_S$

Many studies found that R_S and its isotopic composition are largely controlled by photosynthesis through its impact on root respiration (Steinmann et al. 2004; Göttlicher et al. 2006; Högberg et al. 2008; Bahn et al. 2009). Most of these studies, however, were conducted in dense forests with a high relative root contribution to soil CO_2 efflux. Inversely, lower C allocation to the roots may explain smaller autotrophic respiration fluxes in less productive ecosystems (Subke et al. 2006). Our results for the oak-savannah fit this theory: low R_S rates coincided with a low contribution of roots (15–28%) to R_S, and heterotrophic organisms dominated overall R_S (up to 85%; see Fig. 2i–l).

$\delta^{13}C_{res}$ of both SMO and soil were substantially more depleted than foliage and root respiration (Fig. 3) and exhibited little variation in response to drought. At the end of the observation period $\delta^{13}C_{res}$ values increased slightly.

While R_{SMO} declined with drought by ca. 1 µmol m^{-2} s^{-1}, root respiration remained stable (see Fig. 4), and thus increased its relative contribution to total soil efflux explaining the slight enrichment in $\delta^{13}C_{soil}$ with enhanced drought. However, overall changes in soil $\delta^{13}C_{res}$ were not significant, thus we assume the utilization of a stable C source and only minor influence of photosynthetic discrimination. With increasing drought, diurnal variations in $\delta^{13}C_{res}$ of SMO were found, similar to the pattern in root respiration (see Fig. 3). Soil microbes are known for their ability to assimilate C by anaplerotic CO_2 fixation, where phosphoenolpyruvate carboxylase (PEPc) assimilates CO_2 from the soil air (e.g., Wingler et al. 1996). Through mixing of atmospheric and respired C in the soil air spaces, anaplerosis-derived CO_2 is substantially enriched compared to C input from C_3 plants (Tu and Dawson 2005). Furthermore, through decreased input of photosynthetic assimilates, the C cycle of deeper soil layers is increasingly sustained by soil microbial biomass (Tu and Dawson 2005) and old SOM, thus leading to a more enriched ^{13}C signature (e.g., Paterson et al. 2009). However, it has to be considered that anaplerotic C fixation by PEPc is not an efficient mechanism to sustain respiration under increased drought, but rather might contribute to the generally observed enrichment with deeper soil layers. Under drought conditions, when SMO respiration in the upper soil layers is restrained by low soil moisture, the influence of R_S from deeper soil layers, where soil microbial communities have less access to plant-derived C and are supplied to a larger extent by anaplerotic CO_2 fixation, might become higher and thus result in more enriched $\delta^{13}C_{res}$ of SMO. However, there was no substrate input from plants in the trenching plots and there were no indications as to why the magnitude of anaplerosis-derived CO_2 should be increased at night. More research will be needed to clarify the observed pattern.

Variation in $\delta^{13}C_{res}$ of foliage

With progressing drought R_{eco} and R_S became increasingly similar, indicating a large decrease in canopy respiration (Davidson et al. 2006). In spite of the canopy-scale decrease, dark respiration of single leaves of the understory species *T. guttata* increased strongly (see Fig. 2a–d), which can be attributed to accelerated metabolism in dying tissue. The $\sim$90% decrease in understory respiration (Fig. 4e; see also Unger et al. 2009) at the canopy scale was therefore entirely due to a drought-induced decrease in leaf area. *Q. ilex* on the other hand was able to extract sufficient water from deeper soil layers (e.g., Kurz-Besson et al. 2006; Pereira et al. 2007) and did not respond markedly to drought (Fig. 4c).

During the course of drought $\delta^{13}C_{res}$ decreased by 2.4 ± 1.4 and 5.0 ± 2.0‰ in *Q. ilex* and *T. guttata* leaves,

respectively (see Fig. 3). In contrast, controlled experiments found more enriched $\delta^{13}C_{res}$ in drought-stressed plants as compared to controls, as drought-induced decreases in photosynthetic discrimination resulted in enriched substrates and thus increasing $\delta^{13}C_{res}$ (Duranceau et al. 1999). However, under natural conditions drought is accompanied by increasing temperatures and VPD. In accordance with our findings, Tcherkez et al. (2003) showed that increasing temperatures led to more depleted $\delta^{13}C_{res}$. Further, old C sources may contribute more than 50% to overall respiration (Nogués et al. 2006). When respiratory demand exceeds C input during drought, C from more depleted C sources will be respired, particularly at night when assimilate pools decline, which was probably the case in *T. guttata*. Thus, increased respiratory substrate demand in combination with decreasing C fixation may induce the utilization of more depleted sources (e.g., fatty acids; see also Duranceau et al. 1999).

Further, substantial post-photosynthetic fractionation during dark respiration of foliage has been observed (Ghashghaie et al. 2003), which can be explained by heterogeneous distribution of heavy C within hexose molecules (Rossmann et al. 1991; Gleixner and Schmidt 1997). This intramolecular heterogeneity of ^{13}C results in an 'apparent fractionation' during dark respiration depending on the balance between pyruvate dehydrogenase and Krebs cycle metabolic reactions due to the deviation of C to secondary metabolism (Tcherkez et al. 2003; Ghashghaie et al. 2003; Werner et al. 2007b; 2009; Priault et al. 2009). The observed depletion in foliage $\delta^{13}C_{res}$ with drought (Fig. 3a–h) might, therefore, be explained by decreasing investment into secondary metabolism in response to decreasing C supply versus increasing C demand. Post-photosynthetic fractionation may also be responsible for the marked diurnal dynamics in foliage $\delta^{13}C_{res}$ (especially in *T. guttata*) with increasing enrichment during the light period and subsequent depletion after dark (Hymus et al. 2005; Prater et al. 2006; Werner et al. 2007b, 2009; Priault et al. 2009). It was shown that strongest diurnal enrichment occurred in species with enhanced investment into secondary metabolism as well as increased maintenance versus growth respiration (Werner et al. 2007b, 2009; Priault et al. 2009). In contrast to these studies under controlled conditions, diurnal variability was larger in the fast-growing *T. guttata* than in the evergreen *Q. ilex* and increased with enhanced drought. Thus, we hypothesize that changes in $\delta^{13}C_{res}$ of *T. guttata* were due to substantial substrate changes rather than a response in post-photosynthetic fractionation. On the other hand, in *Q. ilex* drought might have caused decreasing investment in secondary metabolism, explaining the decrease in diurnal amplitude of $\delta^{13}C_{res}$ variations. Hence, under drought and low C assimilation, substrate changes and post-photosynthetic

fractionation effects masked the rather small effects of photosynthetic discrimination on $\delta^{13}C_{res}$ of the studied Mediterranean species.

Recently, $\delta^{13}C_{res}$ has been shown to be markedly ^{13}C enriched during the first minutes of darkness after illumination (e.g., Mortazavi et al. 2006; Gessler et al. 2009b; Werner et al. 2009), mainly in light-acclimated leaves, compared with the more depleted steady state of dark-adapted leaves. This was explained by light-enhanced dark respiration (LEDR) that would originate from the use of organic acids (e.g., malate) as respiratory substrates (e.g., Gessler et al. 2009b; Barbour and Hanson 2009; Werner et al. 2009). Hence, LEDR might play a role in the observed enrichment of daytime respiration in foliage. The extent to which rapid post-illumination changes are involved in diurnal dynamics in $\delta^{13}C_{res}$ is largely unclear (Werner et al. 2009). However, Werner et al. (2009) showed that diurnal dynamics in $\delta^{13}C_{res}$ occur independently from the rapid post-illumination dynamics. Moreover, they showed that time series of post-illumination $\delta^{13}C_{res}$ measurements in $Q.~ilex$ leaves undergo diurnal enrichment of comparable magnitudes, when comparing the same times of dark adaptation. Incubation time of our samples in the dark was in all cases 10 min, thus providing comparable conditions. Furthermore, main shifts in leaf $\delta^{13}C_{res}$ occurred during nighttime, when LEDR does not occur. Therefore, we suggest that LEDR only played a minor role explaining the observed daytime dynamics in foliage $\delta^{13}C_{res}$.

Variation in $\delta^{13}C_r$

Root respiration contributed only marginally to R_{eco} (<10%), and remained stable even with senescence of aboveground biomass, which might be due to the C storage function of roots (e.g., Pregitzer et al. 2000). Metabolic processes of root respiration are not yet well understood (Barbour and Hanson 2009). Many laboratory studies (Klumpp et al. 2005; Badeck et al. 2005; Bathellier et al. 2008, 2009; Gessler et al. 2009b; Barbour and Hanson 2009) under well-watered conditions have shown that root respiration is slightly more depleted than shoot respiration. This was generally explained with anaplerotic CO_2 fixation. Like SMO, roots contain PEPc, which fractionates in favor of ^{13}C (Klumpp et al. 2005) and thus metabolizes enriched CO_2, re-fixed from the root respiration flux, resulting in more depleted respiration. In contrast to these studies, root respired $\delta^{13}CO_2$ of $T.~guttata$ became increasingly enriched under severe drought, whereas the opposite pattern was observed in leaves. As PEPc does not use gaseous CO_2 but HCO_3^- in the liquid phase (Mohr and Schopfer 1992) and thus is directly moisture dependent, a drought-induced reduction in PEPc activity might be a

likely explanation for the increased enrichment in root $\delta^{13}C_{res}$. However, the influence of PEPc on respiratory metabolism in roots may be highly species dependent. Bathellier et al. (2009) found no marked effect of PEPc on $\delta^{13}C_{res}$ of roots in $Phaseolus~vulgaris$, whereas Gessler et al. (2009b) reported large effects in $Ricinus~communis$.

Similar to our results, other studies found root (Gessler et al. 2007) as well as trunk respired CO_2 (Damesin and Lelarge 2003; Brandes et al. 2006) to be ^{13}C enriched as compared to the putative substrates (Cernusak et al. 2009). Gessler et al. (2007) found a marked nocturnal enrichment in $\delta^{13}C$ of $Eucalyptus$ phloem sap, probably due to fractionation during nocturnal starch remobilization. Fructose produced from starch break-down is isotopically heavier than sucrose produced in the light (Gleixner et al. 1998). Gleixner et al. (1998) also showed that tuber sucrose of potato plants appeared to be significantly enriched compared with leaf sucrose. $T.~guttata$ also produces tubers for enhanced carbohydrate storage. Thus, a nocturnal substrate change from freshly produced hexose to stored starch might explain the observed nocturnal enrichment.

Variation in $\delta^{13}C_R$

Despite the strong decrease in R_{eco}, $\delta^{13}C_R$ did not undergo marked temporal variations with drought (e.g., McDowell et al. 2004b; Lai et al. 2005; Ponton et al. 2006), though exhibiting large diurnal shifts (e.g., Bowling et al. 2003; Werner et al. 2006; Kodama et al. 2008). Flux partitioning indicated that changes in isotopic composition of R_{eco} occur mainly upon changes in the relative contribution of component fluxes with different isotopic signatures. Similar to Tang and Baldocchi (2005) the pattern of R_{eco} was mainly driven by soil moisture but the diurnal pattern was controlled by temperature (see Unger et al. 2009). A main contributor to R_{eco} was R_S (ca. 60–80% of R_{eco}), while canopy respiration constituted a smaller flux (20–40%); these ranges are comparable to those of other studies (e.g., Goulden et al. 1996; Lavigne et al. 1997; Law et al. 2001; Davidson et al. 2006). The R_S flux (particularly that of SMO) thus had the largest influence on $\delta^{13}C_R$, with both $\delta^{13}C_R$ and $\delta^{13}C_{soil}$ being more depleted compared to other ecosystem components.

Seasonal variations in $\delta^{13}C_R$ and $\delta^{13}C_{soil}$ have been linked to meteorological events via their effects on canopy discrimination and substrate supply to root respiration (Ekblad and Högberg 2001; Bowling et al. 2002; McDowell et al. 2004b; Knohl et al. 2005; Mortazavi et al. 2005; Werner et al. 2006; Alstad et al. 2007; Högberg et al. 2008) and even to a drought-induced increase in ecosystem-scale water use efficiency (Ponton et al. 2006). However, such relations were not observed in this study: mean nocturnal $\delta^{13}C_R$ remained relatively stable with increasing VPD and

T_{air}, which was in agreement with gas exchange measurements, indicating only a minor drought response of tree photosynthetic discrimination (*Q. ilex*; Table 1). Assimilates of the vanishing understory (e.g., *T. guttata*) probably also played a minor role in $\delta^{13}C_R$ as the fluxes declined rapidly.

Large shifts in $\delta^{13}C_R$ (6‰) were found within the nocturnal cycle. Unexpectedly, however, these variations did not show a strong relationship with diurnal variations in the different component fluxes, as derived from a comparison of measured and eco-isoflux calculated values (see Fig. 3m–p).

The major problem here seems to be the applicability of the Keeling plot method at the ecosystem scale. Given the large differences between the $\delta^{13}C_{res}$ of the component fluxes from soil, roots and foliage the sampling method of a vertical gradient may conflict with the law of a constant source flux signature, and thus produce bias in the two-source mixing model. Further, Schaeffer et al. (2008) showed that canopy structure and differences in atmospheric mixing might introduce a bias into Keeling plot estimates sampled over a height gradient. They found that $\delta^{13}C_R$ sampled at canopy height correlated with time-lagged VPD, while $\delta^{13}C_R$ sampled at ground level correlated with soil moisture. These correlations became stronger when sampling periods with strong mixing of ground and canopy air were excluded, suggesting that atmospheric dynamics play a large role in the estimate of $\delta^{13}C_R$. Finally, it is known that small CO_2 gradients (below 30 p.p.m.) can reduce confidence in the estimate of $\delta^{13}C_R$ (Pataki et al. 2003; Zobitz et al. 2006). Indeed, CO_2 gradients obtained for ecosystem Keeling plots were on average only 36 p.p.m. Hence, $\delta^{13}C_R$ results need to be considered with care. Nevertheless, the lowest nocturnal variability in $\delta^{13}C_R$ was found on 3 June, when the $\delta^{13}C_{res}$ of foliage and R_S were most similar. This is in agreement with the hypothesis that changes in both signatures and relative contributions from the components may result in temporal shifts in $\delta^{13}C_R$ (for a thorough discussion see Werner et al. 2006).

Validity of isotopic partitioning approaches

While no study has yet measured the $\delta^{13}C$ values of all major ecosystem components simultaneously for $\delta^{13}C_R$, a few have measured several of these fluxes at once (Bowling et al. 2003; McDowell et al. 2004a; Mortazavi et al. 2005; Kodama et al. 2008); however, so far none of them has achieved mass balance (Bowling et al. 2008). Here, we attempted to close an isotopic flux mass balance at both ecosystem (eco-isoflux) and soil scales (soil-isoflux). At the soil scale (soil-isoflux) both partitioning approaches revealed good agreement (see Table 2; Fig. 4). However,

we did not manage to close the mass balance at the ecosystem scale: especially when calculating small fluxes, the eco-isoflux and ecoflux approach showed somewhat large deviations (see Table 2; Fig. 4). Only when calculating R_{eco} from the ecosystem component fluxes and their isotopic compositions did we find good agreement with measured R_{eco}.

Apart from a methodical bias potentially associated with the flux measurements (e.g., pressure gradients in the soil chambers and the trenching approach; for a thorough discussion see Unger et al. 2009), there might be several reasons for the inability to close the eco-isoflux mass balance:

Firstly, there was good agreement of measured and calculated R_{eco} in contrast to the somewhat large deviations of the component fluxes derived from the eco-isoflux approach. This indicates that, as discussed above, the Keeling plot measurements at the ecosystem scale were a large source of error in the eco-isoflux approach. At the soil scale, on the other hand, soil-isoflux partitioning showed good agreement with the soilflux estimates, since Keeling plots were more reliable because: (1) they were sampled using a well-mixed chamber system, thus eliminating the problems involved in sampling over a height gradient with different components signatures; (2) CO_2 gradients were generally large (~ 80 p.p.m.); and (3) at the soil scale atmospheric dynamics are less important, as the soil chamber acts as a closed system.

Another potential source of error in the eco-isoflux approach might have been a missing flux. All main ecosystem components and their respective $\delta^{13}C_{res}$ were measured, apart from stem and branch respiration from the trees that were included in the tree flux. Sensitivity analyses revealed that the addition of a small flux with natural signatures expected from stem and branch respiration would not change the results of the mass balance significantly. However, only a small flux with a very negative isotopic signature (e.g., from fossil fuel combustion) might explain differences in measured and calculated $\delta^{13}C_R$ (data not shown). On the contrary, for R_S, a scale with fewer contributing components, the soil-isoflux approach worked very well.

Potential bias might have been introduced by using isotopic compositions from single leaves and root respiration as representative of the isotopic compositions of the understory, tree and root fluxes, resulting in error in the fluxes estimated by the eco-isoflux approach. Further, the understory flux data might have introduced error into R_u estimates as these were from a grassland site adjacent to the studied oak forest (although they had similar conditions). However, these errors are expected to be minor as trees are widely spaced in the forest site and soil measurements for the understory flux partitioning were taken in the large

areas between trees, where energy balance and understory flux are expected to be similar to those in the grassland site. Further, the seasonality of understory growth patterns is comparable between the two sites (Pereira et al. 2007) and somewhat different management and species composition did not largely affect the comparability of the understory fluxes from the different systems (see "Materials and methods") during the study period.

Conclusion

Stables isotope ratios of ecosystem component fluxes carry valuable information on regulatory processes of an ecosystem's response to drought. Large and rapid dynamics in isotopic compositions of foliage, root and soil respiratory fluxes were most probably due to: (1) post-photosynthetic fractionation, (2) changes in respired substrates, (3) drought-induced changes in PEPc activity, and (4) an increased relative contribution of R_S from deeper soil layers with drought—effects masking the imprint of photosynthetic discrimination on $\delta^{13}CO_2$ of both components and R_{eco}.

We did not manage to fully close an isotope-based mass balance at the ecosystem scale, mainly due to uncertainties regarding ecosystem Keeling plots. However, promising results were achieved at the soil scale, indicating that isotopic mass balance works well under conditions of high CO_2 gradients and stable sampling conditions.

Nevertheless, $\delta^{13}C_R$ is an important parameter in isotope-based C budget models and for an understanding of the controls over terrestrial C exchange processes. Thus, future research should focus on the achievement of improved methodology to measure or model $\delta^{13}C_R$ for mass balance approaches and to quantify the underlying processes of short-term dynamics of the isotopic composition of R_{eco}.

References

Aires LM, Pio CA, Pereira JS (2008) The effect of drought on energy and water vapour exchange above a Mediterranean C3/C4 grassland in Southern Portugal. Agric For Meteorol 148:565–579

Alstad KP, Lai C-T, Flanagan LB, Ehleringer JR (2007) Environmental controls on the carbon isotope composition of ecosystem-respired CO_2 in contrasting forest ecosystems in Canada and the USA. Tree Physiol 27:1361–1374

Badeck F, Tcherkez G, Nogués S, Piel C, Ghashghaie J (2005) Post-photosynthetic fractionation of stable carbon isotopes between plant organs—a widespread phenomenon. Rapid Commun Mass Spectrom 19:1381–1391

Bahn M, Schmitt M, Siegwolf R, Richter A, Brüggemann N (2009) Does photosynthesis affect grassland soil respired CO_2 and its carbon isotope composition on a diurnal timescale? New Phytol 182:451–460

Barbour M, Hanson DT (2009) Stable carbon isotopes reveal dynamics of respiratory metabolism. New Phytol 181:243–245

Bathellier C, Badeck F, Couzi P, Harscoet S, Mauve C, Ghashghaie J (2008) Divergence in $\delta^{13}C$ of dark respired CO_2 and bulk organic matter occurs during the transition between heterotrophy and autotrophy in *Phaseolus vulgaris* plants. New Phytol 177:406–418

Bathellier C, Tcherkez G, Bligny R, Grout E, Cornic G, Ghashghaie J (2009) Metabolic origin of the ^{13}C of respired CO_2 in roots of *Phaseolus vulgaris*. New Phytol 181:387–399

Bowling DR, Tans PP, Monson RK (2001) Partitioning net ecosystem carbon exchange with isotopic fluxes of CO_2. Glob Chang Biol 7:127–145

Bowling DR, McDowell NG, Bond BJ, Law BE, Ehleringer JR (2002) ^{13}C content of ecosystem respiration is linked to precipitation and vapor pressure deficit. Oecologia 131:113–124

Bowling DR, Sargent SD, Tanner BD, Ehleringer JR (2003) Tunable diode laser absorption spectroscopy for stable isotope studies of ecosystem-atmosphere CO_2 exchange. Agric For Meteorol 118:1–19

Bowling DR, Pataki DE, Randerson JT (2008) Carbon isotopes in terrestrial ecosystem pools and CO_2 fluxes. New Phytol 178:24–40

Brandes E, Kodama N, Whittaker K, Weston C, Rennenberg H, Keitel C, Adams MA, Gessler A (2006) Short-term variation in the isotopic composition of organic matter allocated from the leaves to the stem of *Pinus sylvestris*: effects of photosynthetic and post-photosynthetic carbon isotope fractionation. Glob Chang Biol 12:1922–1939

Carreiras JMB, Pereira JMC, Pereira JS (2006) Estimation of tree canopy cover in evergreen oak woodlands using remote sensing. For Ecol Manage 223:45–53

Cernusak LA, Tcherkez G, Keitel C, Cornwell WK, Santiago LS, Knohl A, Barbour MM, Williams DG, Reich PB, Ellsworth DS, Dawson TE, Griffiths HG, Farquhar GD, Wright IJ (2009) Why are non-photosynthetic tissues generally ^{13}C enriched compared with leaves in C3 plants? Review and synthesis of current hypotheses. Funct Plant Biol 36:199–213

Damesin C, Lelarge C (2003) Carbon isotope composition of current-year shoots from *Fagus sylvatica* in relation to growth, respiration and use of reserves. Plant Cell Environ 26:207–219

Davidson EA, Richardson AD, Savage KE, Hollinger DY (2006) A distinct seasonal pattern of the ratio of soil respiration to total ecosystem respiration in a spruce-dominated forest. Glob Chang Biol 12:230–239

Duranceau M, Ghashghaie J, Badeck F, Deléens E, Cornic G (1999) $\delta^{13}C$ of leaf carbohydrates in relation to dark respiration in *Phaseolus vulgaris* L. under progressive drought. Plant Cell Environ 22:515–523

Ekblad A, Högberg P (2001) Natural abundance of ^{13}C in CO_2 respired from forest soils reveals speed of link between photosynthesis and root respiration. Oecologia 127:305–308

Ekblad A, Bostrom B, Holm A, Comstedt D (2005) Forest soil respiration rate and delta C-13 is regulated by recent above ground weather conditions. Oecologia 143:136–142

Gessler A, Keitel C, Kodama N, Weston C, Winters AJ, Keith H, Grice K, Leuning R, Farquhar GD (2007) $\delta^{13}C$ of organic matter transported from the leaves to the roots in *Eucalyptus*

delegatensis: short-term variations and relation to respired CO_2. Funct Plant Biol 34:692–706

Gessler A, Brandes E, Buchmann N, Helle G, Rennenberg H, Barnard RL (2009a) Tracing carbon and oxygen isotope signals from newly assimilated sugars in the leaves to the tree-ring archive. Plant Cell Environ 32:780–795

Gessler A, Tcherkez G, Karyanto O, Ferrio JP, Ghashghaie J, Kreuzwieser J, Farquhar GD (2009b) On the metabolic origin of the carbon isotope composition of CO_2 evolved from darkened light-acclimated leaves in *Ricinus communis*. New Phytol 181:374–386

Ghashghaie J, Badeck F, Lanigan G, Nogúes S, Tcherkez G, Deléens E, Cornic G, Griffiths H (2003) Carbon isotope fractionation during dark respiration and photorespiration in C3 plants. Phytochem Rew 2:145–161

Gleixner G, Schmidt H-L (1997) Carbon isotope effects on the fructose-1, 6-bisphosphate aldolase reaction, origin for non-statistical ^{13}C distributions in carbohydrates. J Biol Chem 272:5382–5387

Gleixner G, Scrimgeour C, Schmidt H-L, Viola R (1998) Stable isotope distribution in the major metabolites of source and sink organs of *Solanum tuberosum* L.: a powerful tool in the study of metabolic partitioning in intact plants. Planta 207:241–245

Göttlicher SG, Steinmann K, Betson NR, Hogberg P (2006) The dependence of soil microbial activity on recent photosynthate from trees. Plant Soil 287:85–94

Goulden ML, Munger JW, Fan SM, Daube BC, Wofsy SC (1996) Measurements of carbon sequestration by long-term eddy covariance: methods and a critical evaluation of accuracy. Glob Chang Biol 2:169–182

Griffis TJ, Black TA, Gaumont-Guay D, Drewitt GB, Nesic Z, Barr AG, Morgenstern K, Kljun N (2004) Seasonal variation and partitioning of ecosystem respiration in a southern boreal aspen forest. Agric For Meteorol 125:207–223

Högberg P, Högberg MN, Göttlicher SG, Betson NR, Keel SG, Metcalfe DB, Campbell C, Schindlbacher A, Hurry V, Lundmark T, Linder S, Näsholm T (2008) High temporal resolution tracing of photosynthate carbon from the tree canopy to forest soil microorganisms. New Phytol 177:120–128

Huxman TE, Turnipseed AA, Sparks JP, Harley PC, Monson RK (2003) Temperature as a control over ecosystem CO_2 fluxes in a high-elevation, subalpine forest. Oecologia 134:537–546

Hymus GJ, Maseyk K, Valentini R, Yakir D (2005) Large daily variation in ^{13}C-enrichment of leaf-respired CO_2 in two *Quercus* forest canopies. New Phytol 167:377–384

Keeling CD (1958) The concentration and isotopic abundance of atmospheric carbon dioxide in rural areas. Geochim Cosmochim Acta 13:322–334

Klumpp K, Schäufele R, Lötscher M, Lattanzi FA, Feneis W, Schnyder H (2005) C-isotope composition of CO_2 respired by shoots and roots: fractionation during dark respiration. Plant Cell Environ 28:241–250

Knohl A, Werner RA, Brand WA, Buchmann N (2005) Short-term variations in $\delta^{13}C$ of ecosystem respiration reveals link between assimilation and respiration in a deciduous forest. Oecologia 142:70–82

Kodama N, Barnard R, Salmon Y, Weston C, Ferrio JP, Holst J, Werner RA, Saurer M, Rennenberg H, Buchmann N, Gessler A (2008) Temporal dynamics of the carbon isotope composition in a *Pinus sylvestris* stand: from newly assimilated organic carbon to respired carbon dioxide. Oecologia 156:737–750

Kurz-Besson C, Otieno DO, Lobo do Vale R, Siegwolf R, Schmidt M, Herd A, Nogueira C, David TS, David JS, Tenhunen J, Pereira JS, Chaves M (2006) Hydraulic lift in cork oak trees in a savannah-type Mediterranean ecosystem and its contribution to the local water balance. Plant Soil 282:361–378

Lai CT, Ehleringer JR, Schauer AJ, Tans PP, Hollinger DY, Paw U, Munger JW, Wofsy SC (2005) Canopy-scale delta ^{13}C of photosynthetic and respiratory CO_2 fluxes: observations in forest biomes across the United States. Glob Chang Biol 11:633–643

Lavigne MB, Ryan MG, Anderson DE, Baldocchi DD, Crill PM, Fitzjarrald DR, Goulden ML, Gower ST, Massheder JM, McCaughey JH, Rayment M, Striegl RG (1997) Comparing nocturnal eddy covariance measurements to estimates of ecosystem respiration made by scaling chamber measurements at six coniferous boreal sites. J Geophys Res Atmos 102:28977–28985

Law BE, Goldstein AH, Anthoni PM, Unsworth MH, Panek JA, Bauer MR, Fracheboud JM, Hultman N (2001) Carbon dioxide and water vapor exchange by young and old ponderosa pine ecosystems during a dry summer. Tree Physiol 21:299–308

Lee MS, Nakane K, Nakatsubo T, Koizumi H (2003) Seasonal changes in the contribution of root respiration to total soil respiration in a cool-temperate deciduous forest. Plant Soil 255:311–318

McDowell NG, Bowling DR, Bond BJ, Irvine J, Law BE, Anthoni P, Ehleringer JR (2004a) Response of the carbon isotopic content of ecosystem, leaf, and soil respiration to meteorological driving factors in a *Pinus ponderosa* ecosystem. Glob Biogeochem Cycles GB1013. doi:10.1029/2003GB002049

McDowell NG, Bowling DR, Schauer A, Irvine J, Bond BJ, Law BE, Ehleringer JR (2004b) Associations between carbon isotope ratios of ecosystem respiration, water availability and canopy conductance. Glob Chang Biol 10:1767–1784

Mohr H, Schopfer P (1992) Plant physiology, 4th edn. Springer, New York

Mortazavi B, Chanton JP, Prater JL, Oishi AC, Oren R, Katul G (2005) Temporal variability in ^{13}C of respired CO_2 in a pine and a hardwood forest subject to similar climatic conditions. Oecologia 142:57–69

Mortazavi B, Chanton JP, Smith MC (2006) Influence of C-13-enriched foliage respired CO_2 on delta C-13 of ecosystem-respired CO_2. Glob Biogeochem Cycles 20:GB3029. doi:10.1029/2005GB002650

Nogués S, Damesin C, Tcherkez G, Maunoury F, Cornic G, Ghashghaie J (2006) $^{13}C/^{12}C$ isotope labelling to study leaf carbon respiration and allocation in twigs of field grown beech trees. Rapid Commun Mass Spectrom 20:219–226

Ogée J, Peylin P, Ciais P, Bariac T, Brunet Y, Berbigier P, Roche C, Richard P, Bardoux G, Bonnefond JM (2003) Partitioning net ecosystem carbon exchange into net assimilation and respiration using $^{13}CO_2$ measurements: a cost-effective sampling strategy. Global Biogeochemical Cycles 17:1070, doi:10.1029/2002GB001995

Pataki DE, Ehleringer JR, Flanagan LB, Yakir D, Bowling DR, Still CJ, Buchmann N, Kaplan JO, Berry JA (2003) The application and interpretation of Keeling plots in terrestrial carbon cycle research. Glob Biogeochem Cycles 17:1022. doi:10.1029/2001GB001850

Paterson E, Midwood AJ, Millard P (2009) Through the eye of the needle: a review of isotope approaches to quantify microbial processes mediating soil carbon balance. New Phytol 184:19–33

Pereira JS, Mateus JA, Aires LM, Pita G, Pio C, David JS, Andrade V, Banza J, David TS, Paço TA, Rodrigues A (2007) Net ecosystem carbon exchange in three contrasting Mediterranean ecosystems. The effect of drought. Biogeosciences 4:791–802

Ponton S, Flanagan LB, Alstad KP, Johnson BG, Morgenstern K, Kljun N, Black TA, Barr AG (2006) Comparison of ecosystem water-use efficiency among Douglas-fir forest, aspen forest and grassland using eddy covariance and carbon isotope techniques. Glob Chang Biol 12:294–310

Prater JL, Mortazavi B, Chanton JP (2006) Diurnal variation of the $\delta^{13}C$ of pine needle respired CO_2 evolved in darkness. Plant Cell Environ 29:202–211

Pregitzer KS, King JA, Burton AJ, Brown SE (2000) Responses of tree fine roots to temperature. New Phytol 147:105–115

Priault P, Wegener F, Werner C (2009) Pronounced differences in diurnal variation of carbon isotope composition of leaf respired CO_2 among functional groups. New Phytol 181:400–412

Reichstein M, Falge E, Baldocchi D, Papale D, Aubinet M, Berbigier P, Bernhofer C, Buchmann N, Gilmanov T, Granier A, Grunwald T, Havrankova K, Ilvesniemi H, Janous D, Knohl A, Laurila T, Lohila A, Loustau D, Matteucci G, Meyers T, Miglietta F, Ourcival JM, Pumpanen J, Rambal S, Rotenberg E, Sanz M, Tenhunen J, Seufert G, Vaccari F, Vesala T, Yakir D, Valentini R (2005) On the separation of net ecosystem exchange into assimilation and ecosystem respiration: review and improved algorithm. Glob Chang Biol 11:1424–1439

Rossmann A, Butzenlechner M, Schmidt HL (1991) Evidence for a non-statistical carbon isotope distribution in natural glucose. Plant Physiol 96:609–614

Schaeffer SM, Anderson DE, Burns SP, Monson RK, Sun J, Bowling DR (2008) Canopy structure and atmospheric flows in relation to the $\delta^{13}C$ of respired CO_2 in a subalpine coniferous forest. Agric For Meteorol 148:592–605

Schnyder H, Schaufele R, Wenzel R (2004) Mobile, outdoor continuous-flow isotope-ratio mass spectrometer system for automated high-frequency C-13- and O-18-CO_2 analysis for Keeling plot applications. Rapid Commun Mass Spectrom 18:3068–3074

Steinmann KTW, Siegwolf R, Saurer M, Korner C (2004) Carbon fluxes to the soil in a mature temperate forest assessed by C-13 isotope tracing. Oecologia 141:489–501

Still CJ, Berry JA, Ribas-Carbó M, Helliker BR (2003) The contribution of C_3 and C_4 plants to the carbon cycle of tallgrass prairie: an isotopic approach. Oecologia 136:347–359

Subke JA, Inglima I, Cotrufo MF (2006) Trends and methodological impacts in soil CO_2 efflux partitioning: a metaanalytical review. Glob Chang Biol 12:921–943

Sun W, Resco V, Williams D (2009) Diurnal and seasonal variation in the carbon isotope composition of leaf dark-respired CO_2 in velvet mesquite (Prosopis velutina). Plant Cell Environ 32:1390–1400

Tang JW, Baldocchi DD (2005) Spatial and temporal variation in soil respiration in an oak-grass savannah ecosystem in California and its partitioning into autotrophic and heterotrophic components. Biogeochemistry 73:183–207

Tcherkez G, Nogués S, Bleton J, Cornic G, Badeck F, Ghashghaie J (2003) Metabolic origin of carbon isotope composition of leaf dark-respired CO_2 in French bean. Plant Physiol 131:237–244

Tcherkez G, Farquhar G, Badeck F, Ghashghaie J (2004) Theoretical considerations about carbon isotope distribution in glucose of C3 plants. Funct Plant Biol 31:857–877

Tenhunen JD, Sala Serra A, Harley PC, Dougherty RL, Reynolds FJ (1990) Factors influencing carbon fixation and water use by Mediterranean sclerophyll shrubs during summer drought. Oecologia 82:381–393

Tu KP, Dawson TE (2005) Partitioning ecosystem respiration using stable carbon isotope analyses of CO_2. In: Flanagan L, Ehleringer JR, Pataki DE (eds) Stable isotopes and biosphere-atmosphere interactions. Elsevier Academic Press, San Diego, pp 125–148

Unger S, Máguas C, Pereira JS, Aires LM, David TS, Werner C (2009) Partitioning carbon fluxes in a Mediterranean oak forest to disentangle changes in ecosystem sink strength during drought. Agric For Meteorol 149:949–961

Valentini R, Matteucci G, Dolman AJ, Schulze E-D, Rebmann C, Moors EJ, Granier A, Gross P, Jensen NO, Pilegaard K (2000) Respiration as the main determinant of carbon balance in European forests. Nature 404:861–865

Werner C, Correia O (1996) Photoinhibition in cork-oak leaves under stress: influence of the bark-stripping on the chlorophyll fluorescence emission in Quercus suber L. Trees 10:288–292

Werner C, Unger S, Pereira JS, Maia R, David TS, Kurz-Besson C, David JS, Maguas C (2006) Importance of short-term dynamics in carbon isotope ratios of ecosystem respiration ($\delta^{13}C_R$) in a Mediterranean oak woodland and linkage to environmental factors. New Phytol 172:330–346

Werner C, Hasenbein N, Maia R, Beyschlag W, Maguas C (2007a) Evaluating high time-resolved changes in carbon isotope ratio of respired CO_2 by a rapid in-tube incubation technique. Rapid Commun Mass Spectrom 21:1352–1360

Werner C, Unger S, Pereira JS, Ghashghaie J, Máguas C (2007b) Temporal dynamics in $\delta^{13}C$ of ecosystem respiration in response to environmental changes. In: Siegwolf R, Dawson TE (eds) Isotopes as tracers of ecological change. Elsevier Academic Press, San Diego, pp 193–210

Werner C, Wegener F, Unger S, Nogués S, Priault P (2009) Short-term dynamics of isotopic composition of leaf respired CO_2 upon darkening: measurements and implications. Rapid Commun Mass Spectrom 23:1–11

Wingler A, Wallenda T, Hampp R (1996) Mycorrhiza formation on Norway spruce (Picea abies) roots affects the pathway of anaplerotic CO_2 fixation. Physiol Plant 96:699–705

Xu LK, Baldocchi DD, Tang JW (2004) How soil moisture, rain pulses, and growth alter the response of ecosystem respiration to temperature. Glob Biogeochem Cycles 18:GB4002.1–GB4002.10

Zobitz JM, Keener JP, Schnyder H, Bowling DR (2006) Sensitivity analysis and quantification of uncertainty for isotopic mixing relationships in carbon cycle research. Agric For Meteorol 136:56–75